



# Signatures of provenance, tectonics and chemical weathering in the Tawi River sediments of the western Himalayan Foreland, India

Mithila Verma<sup>1</sup> · Shyam Kanhaiya<sup>2</sup> · Birendra P. Singh<sup>3</sup> · Saurabh Singh<sup>4,5</sup>

Received: 21 February 2022 / Revised: 11 May 2022 / Accepted: 12 May 2022 / Published online: 1 June 2022  
© The Author(s), under exclusive licence to Springer Nature Switzerland AG 2022

## Abstract

This paper aims to discuss the provenance, tectonics and intensity of chemical weathering and other characteristics of the suspended sediments of the Tawi River located in the Himalayan foreland using geochemical proxies like major, trace and rare earth elements. The Tawi River sediments are primarily to be arkosic in nature with very few litharenite fractions. The compositional variability index (ICV) values range from 0.88 to 1.16 suggesting that the sediments are immature in terms of textural and mineralogical maturity. Major and trace elements data display noticeable depletion of Na<sub>2</sub>O, CaO, MgO, K<sub>2</sub>O, Fe<sub>2</sub>O<sub>3</sub>, Sr and Be relative to upper continental crust (UCC), suggesting alteration of feldspars into clays during progressive weathering in the source area. Enriched Zr, Th and Y relative to UCC suggest occurrence of resistant heavy minerals in the sediments. The chemical index of alteration (CIA), plagioclase index of alteration (PIA), weathering index of Parker (WIP) suggest towards a moderate intensity of chemical weathering in the source area. This is also supported by moderate values of Rb/Sr and K<sub>2</sub>O/Rb ratios of the Tawi River sediments. The chondrite-normalized rare earth element (REE) patterns showing enrichment of light rare earth elements (LREE), nearly flat heavy rare earth elements (HREE) and marked negative Eu anomalies suggest dominance of felsic rocks in the provenance. The other discriminate function diagrams and trace elements ratios (Th/Sc, Zr/Sc and Ti/Zr) and REEs also indicate that the sources of the Tawi River sediments are predominantly felsic in nature. The tectonic signatures of the Tawi River sediments show passive margin setting and humid climatic condition in the source area.

**Keywords** Provenance · Tectonics · Chemical weathering · Suspended sediments · Geochemistry

## 1 Introduction

Weathering of rocks is an important geological phenomenon that has a significant impact on the global carbon cycle and also decreases global temperatures by a few degrees (Dupre et al., 2003). It also reflects on the nature of sediments formed by physical, chemical, and biological processes in response to climate, topography, and source rock characteristics. The geochemistry of the sediments as well as their representation in various plots is very helpful to determine the provenance, tectonics, and source area weathering (Ahmad et al., 2022; Condie et al., 1995; Feng & Kerrich, 1990; Holail & Moghazi, 1998; Nesbitt & Young, 1996; Singh, 2009; Singh & Rajamani, 2001a, b; Taylor & McLennan, 1985; Tripathi & Rajamani, 2003; Tripathy et al., 2014; Wronkiewicz & Condie, 1989). Immobile major and trace elements including Al, Fe, Ti, Th, Sc, Co, Zr, and rare earth elements (REEs) can also be utilised to perceive the source area weathering (Singh, 2009; Taylor & McLennan,

---

Communicated by M. V. Alves Martins

✉ Shyam Kanhaiya  
shyamkanhaiya44@gmail.com

<sup>1</sup> Geoscience/Seismology Division, Ministry of Earth Sciences, New Delhi 110003, India

<sup>2</sup> Department of Earth and Planetary Sciences, V. B. S. Purvanchal University, Jaunpur, UP 222003, India

<sup>3</sup> Department of Geology, Institute of Science, Banaras Hindu University, Varanasi, UP 221005, India

<sup>4</sup> Department of Earth Sciences, IISER, Kolkata, West Bengal 741246, India

<sup>5</sup> Department of Geology, IIES, R. M. L. Avadh University, Ayodhya, UP 224001, India

1985). Because these elements are immobile, they undergo almost nil geochemical fractionation during the weathering processes, so their detailed studies help to understand various geological and weathering processes in the source area (Derry & France-Lanord, 1996; Drever & Zobrist, 1992; Edmond, 1992; Sun et al., 2010). Singh (2010) has postulated that physical weathering and erosion play the dominant role rather than chemical weathering in the Himalayan catchment region of the Ganga River. Also, the REE patterns in suspended and bed-load sediments suggest that the sediments are the result of mechanical crushing of rocks where mineral separation is insignificant (Singh, 2010). In recent decades, notable work on the geochemistry of river sediments have been done in India by Krishnaswami and Singh (2005), Das and Krishnaswami (2007), Sensarma et al. (2008), Singh (2009), Singh (2010), Mondal et al. (2012), Sharma et al. (2013), Kanhaiya et al., (2018a, 2018b), Resmi and Achyuthan (2018) and Bastia et al. (2020).

The present study aimed at exploring the geochemical characteristics of the suspended sediments of the Tawi River to deduce the nature and extent of physical and chemical

weathering in the catchment area, the influence of various processes on sediment geochemistry, their provenance, tectonic setting, and the control of various factors on sediment composition, their maturity and variability. The Tawi River sediments also provide an opportunity to establish an idea about the influence of climate and other exogenic processes on the sediment geochemistry.

## 2 Geology of the area

The Tawi River traverses from the Higher and Lesser Himalayan litho-tectonic units followed by the Sub-Himalayan litho-tectonic units. Metamorphic and igneous rocks of the Higher and Lesser Himalaya occur in the upper reaches and the sedimentary rocks of the Murree and Siwalik groups occur in the lower reaches of the Tawi River catchment (Fig. 1a, b) (Verma et al., 2012). The common rock types in the Higher Himalaya are quartzite, carbonaceous phyllite, crystalline limestone, and felsic schist, followed by porphyroblastic gneiss with alternating quartz-feldspar and biotite

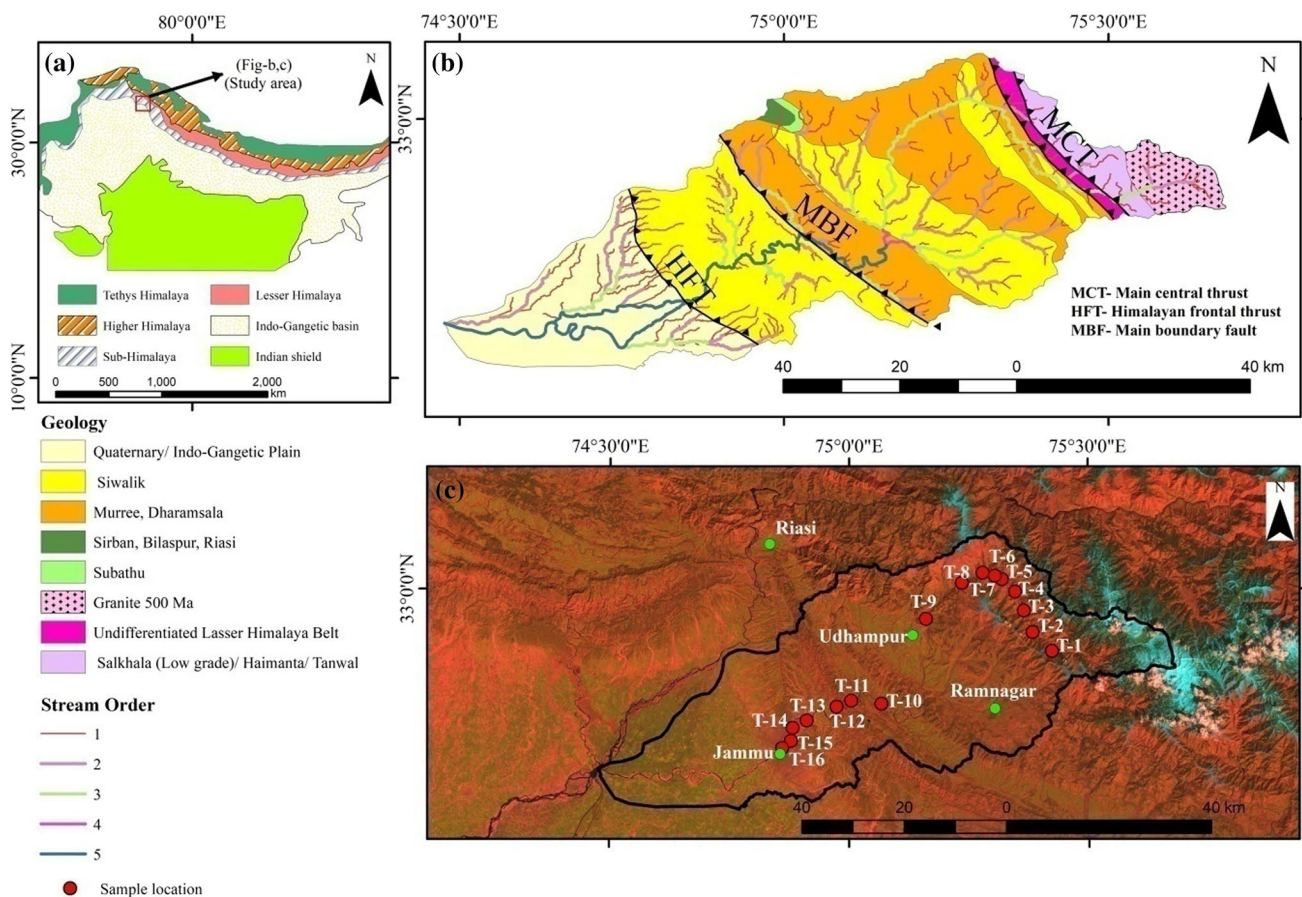


**Fig. 1** a Geological map of the Indian subcontinent showing tectonic sub divisions of the Himalaya (modified after Verma et al. 2012). b Map showing the stream ordering and distributions of different geo-

logical units in the catchment area of the Tawi River Basin (modified after Verma et al. 2012). c Map showing the different sampling locations along the Tawi River

bands. Psammitic gneiss with quartzite, garnetiferous mica schist, porphyroblastic gneiss, and greyish brown gneiss are intercalated with kyanite bands along with tourmaline-bearing granite and biotite granite (Singh, 2007; Thakur et al., 1990). The Main Boundary Thrust separates the Higher Himalaya from the Lesser Himalaya and marks the southern boundary of the Higher Himalaya. The Lesser Himalaya is mostly made up of metamorphic rocks with granite intrusions, and it shows inverted metamorphism, with high-grade rocks lying on top of low-grade rocks (Thakur et al., 1990). High-grade metasedimentary rocks of sillimanite–almandine–orthoclase subfacies demonstrate regional metamorphism of Barrovian–almandine–amphibole facies, and a NNW–SSE trending thrust separates high-grade metamorphic rocks from low-grade metamorphic rocks in the Bhaderwah Rock Formation (Thakur et al., 1990). Garnetiferous-biotite gneisses combined with sillimanite and kyanite schists, marble, and lenticular calc-silicate gneisses make up the metamorphic rocks (Singh, 2007). Acidic and basic intrusive amphibolites, granites, pegmatites, and quartz veins intrude these metasedimentary rocks in some areas. The acidic rocks such as granite and granite gneisses contain zircon and tourmaline in addition to quartz, feldspar and micas. The basic igneous rocks such as Panjal Trap contain augite, andesite and other plagioclase and accessory minerals such as rutile, ilmenite and magnetite. To the south of Lesser Himalaya, the Sub-Himalaya marks its appearance that is bounded by the Main Boundary Thrust (MBT) in the north and the Main Himalayan Thrust (HFT) in the south. The Tertiary sequences in the Jammu area are comprised entirely of the sedimentary rocks (Singh, 2000; Singh et al., 2004). The older sedimentary succession in the Tawi catchment contains mud-pebble conglomerate, sandstone, siltstone and mudstone (Singh, 2000). The younger siliciclastic rocks in the Sub-Himalaya expose a mudstone, sandstone and conglomerate-dominated succession (Singh et al., 2004).

### 3 Tawi River

The Tawi River basin originates in the east of Bhaderwah, in the Indian state of Jammu and Kashmir, from a glaciated terrain having elevation of 4250 m. This glacier is one of several glaciers that occur in the Dhauladhar range of the central Himalaya.

The Tawi catchment lies between 32° 35' and 33° 15' north latitude and 74° 45' and 75° 45' east longitude with a catchment area of 1900 km<sup>2</sup> and drainage of up to fifth order (after Strahler, 1969). The basin's upper section is elongated, whereas the lower section is broad and circular. Rugged rocky terrain dominates the upper reaches of the river, although low hills and aggradational plains dominate

in the lower reaches. The upper reaches of the basin have an east–west slope; whereas the lower reaches have a northeast–southwest slope. The Tawi catchments are divided into three meso-geomorphic zones: the upper one, north of the Panjal Thrust, has a maximum elevation of 4000 m, the middle one, between the Panjal and Udhampur thrusts, has an elevation of 700–1900 m, and the lower one, between Udhampur and Jammu, is made up of low-lying hillocks. Snow feeds only a small fraction of the Tawi catchment, near to its source; on the other hand, the terrain is primarily hilly with plain areas in and around Jammu town and before the Chenab River's confluence. In general, the Tawi River basin has a subtropical monsoonal climate with more active summer monsoon in the plains and winter monsoon in hilly regions. Over the traverses of the Tawi River, the middle reaches experience the more rainfall. The annual rainfall varies from 90 to 140 cm around Bhaderwah town, from 140 to 190 cm over Udhampur, and from 90 to 100 cm over Jammu city.

### 4 Material and methods

Sixteen water samples were collected systematically at definite intervals to extract the suspended load in monsoon season (Fig. 1c). All the sampling points have been mapped (latitude, longitude and elevation) using global positioning system (GPS) (Table. 1). All the samples were collected in polypropylene bottles from the surface (< 10 cm of depth) to avoid sand fraction as the suspended load. Any suspended debris or waste materials were removed from the water samples using a 0.5–mm sieve. The sediments were allowed to

**Table 1** The sampling locations (sample id, latitude, longitude and elevation) of the Tawi River sediment

Sl. no.	Sample id	Latitude	Longitude	Elevation (m)
1.	T-1	75° 25' 25.62"	32° 53' 32.74"	1574 ± 3
2.	T-2	75° 23' 01.11"	32° 55' 33.44"	1385 ± 5
3.	T-3	75° 21' 55.53"	32° 57' 50.55"	1280 ± 2
4.	T-4	75° 20' 49.47"	32° 59' 50.62"	1141 ± 2
5.	T-5	75° 19' 11.67"	33° 01' 08.69"	1064 ± 3
6.	T-6	75° 18' 17.41"	33° 01' 30.68"	1040 ± 4
7.	T-7	75° 16' 44.46"	33° 01' 51.52"	1002 ± 1
8.	T-8	75° 14' 09.08"	33° 00' 46.27"	870 ± 2
9.	T-9	75° 09' 38.47"	32° 56' 59.04"	641 ± 5
10.	T-10	75° 04' 03.34"	32° 48' 00.69"	392 ± 3
11.	T-11	75° 00' 14.43"	32° 48' 20.09"	359 ± 5
12.	T-12	74° 58' 26.40"	32° 47' 41.42"	342 ± 5
13.	T-13	74° 54' 43.29"	32° 46' 15.39"	322 ± 3
14.	T-14	74° 52' 56.06"	32° 45' 26.76"	314 ± 3
15.	T-15	74° 52' 43.46"	32° 44' 05.55"	303 ± 2
16.	T-16	74° 51' 37.45"	32° 43' 19.51"	297 ± 2

settle without disturbing the bottles once they were brought to the laboratory. The water was then decanted to obtain the suspended sediment samples.

To eliminate organic matters, the samples were washed with dilute  $H_2O_2$  and then air dried. Sediment samples were homogenised and then geochemically analysed (Major, Trace and REEs). The X-ray fluorescence (XRF) was used to examine major and trace elements (Philips Universal Vacuum PW1540). Pellets for analysis of major and trace elements were produced according to Stork et al. (1987) and Saini et al. (2000). To validate the precision and accuracy of the sample preparation and instrumental performance, several reference standards were employed, including SO-1, GSS-1, GSS-4, GXR-2, GXR-6, SCO-1, SGR-1, SDO-1, MAG-1, GSD-10, GSR-6 and BCS-267. The measurement precision is ~98% and the measurement accuracy is better than 95% (for details see Purohit et al., 2010). After digestion of the samples in teflon vials with a mixture of  $HF + HNO_3 + HClO_4$  acids according to Shapiro and Brannock (1962) method for solution-B preparation, trace elements, including rare earth elements (REEs) were determined by ICP-MS (Perkin Elmer SCIEX ELAN DRC) (for details see Khanna et al., 2009). Several USGS standards, including SGR-1, MAG-1 and SCO-1, as well as a few in-house standards, were employed to calibrate and validate the results. The precision for the ICP-MS analyses obtained is 95%.

## 5 Results

### 5.1 Geochemistry

The major oxides are presented in Table 2, whereas the trace element concentrations are listed in Table 3 and REEs concentrations are presented in Table 4.

#### 5.1.1 Major oxides

The Tawi River sediments show appreciable variations in the major element concentrations (Table 2). Among the major oxides,  $SiO_2$  shows highest concentration with an average value 69.44 wt% (ranging from 62.4 to 80.3 wt%). The  $SiO_2$  concentration is followed by  $Al_2O_3$  with an average value 12.20 wt%. Other major oxides fall in the range of 12–15 wt% (Table 2). The  $SiO_2/Al_2O_3$  ratio (Avg. = 5.69) of the sediments is greater than Post-Archean Australian Shale (PAAS) value of 3.32 (Taylor & McLennan, 1985) and upper continental crust (UCC) value of 4.33 (Rudnick & GaO, 2014). The  $Al_2O_3$  concentration is followed by  $Fe_2O_3$  with average value 4.91 wt%, with majority of samples lying between 3.23 and 3.96 wt%. The  $TiO_2$  exhibits an average value of 0.62 wt% in the Tawi River sediments. The  $TiO_2$  concentration is followed by CaO with average value 3.00 wt%, with majority of samples lying between 3.20 and 3.76 wt%. The CaO concentration is followed by MgO with average value 1.91 wt%, while the  $K_2O$  content having an average value 2.00 wt%. The concentration of  $Na_2O$  having an average value 0.74 wt% is ranging from 0.57 to 0.85 wt%. The concentration of other oxides is very low, i.e., MnO having average value 0.07 wt% and  $P_2O_5$  having average value 0.08 wt% in the Tawi River sediments.

**Table 2** Estimated major element (in wt%) concentration in ppm for the Tawi River sediments

Sample no.	T-1	T-2	T-3	T-4	T-5	T-6	T-7	T-8	T-9	T-10	T-11	T-12	T-13	T-14	T-15	T-16	Avg
$SiO_2$	80.30	75.06	74.95	70.50	71.08	69.64	69.72	69.34	69.68	68.00	68.11	67.97	68.03	62.37	63.50	62.85	69.44
$TiO_2$	0.52	0.68	0.65	0.65	0.66	0.65	0.65	0.66	0.63	0.66	0.67	0.63	0.65	0.66	0.62	0.65	0.64
$Al_2O_3$	7.77	9.86	10.32	11.25	11.40	11.41	12.21	13.00	12.49	11.97	13.23	12.46	13.17	15.09	14.63	15.02	12.20
$Fe_2O_3$	3.23	3.49	3.35	3.6	3.74	3.78	4.14	4.11	4.34	3.96	3.92	3.84	3.9	5.05	4.92	5.98	4.08
CaO	1.85	1.43	1.14	3.65	3.43	3.20	2.80	2.73	2.82	3.76	3.65	3.70	3.71	3.46	3.29	3.33	3.00
MgO	1.12	1.42	1.53	1.68	1.71	1.69	1.77	1.84	2.00	2.11	2.20	2.17	2.09	2.47	2.40	2.44	1.91
MnO	0.08	0.07	0.07	0.06	0.06	0.06	0.07	0.08	0.07	0.07	0.08	0.07	0.07	0.08	0.07	0.08	0.07
$Na_2O$	0.85	0.57	0.71	0.62	0.64	0.64	0.78	0.70	0.62	0.91	0.87	0.95	0.92	0.65	0.70	0.67	0.74
$K_2O$	1.47	1.64	1.76	1.79	1.90	1.84	2.02	2.00	1.98	1.95	1.90	1.98	1.94	2.63	2.58	2.63	2.00
$P_2O_5$	0.08	0.09	0.10	0.09	0.09	0.09	0.10	0.09	0.09	0.08	0.08	0.01	0.09	0.09	0.09	0.09	0.08
Total	97.27	94.31	94.58	93.89	94.71	93.00	94.26	94.55	94.72	93.47	94.71	93.78	94.57	92.55	92.80	93.75	94.18
CIA	63.33	73.48	71.13	73.83	73.68	74.17	71.86	74.70	74.87	70.06	73.03	70.52	71.67	75.57	74.48	74.62	72.56
PIA	69.2	82.1	79.1	82.8	82.4	82.5	80.3	83.1	84.3	76.9	79.8	76	78.8	85.7	84.3	85.3	80.9
ICV	1.16	0.94	0.88	1.06	1.06	1.03	0.99	0.93	0.99	1.11	0.99	1.06	1.00	0.99	0.99	1.04	1.01



**Table 3** Estimated trace elements concentration (in mg kg<sup>-1</sup>) for the Tawi River sediments

Sample no.	T-1	T-2	T-3	T-4	T-5	T-6	T-7	T-8	T-9	T-10	T-11	T-12	T-13	T-14	T-15	T-16	Avg
Sc	8	8	8	12	10	10	29	25	24	23	24	31	27	25	28	27	19.93
Co	10	11	11	11	12	12	13	11	10	12	14	12	13	11	13	12	11.75
Ni	19	17	22	25	25	29	50	40	38	36	42	40	46	49	44	41	35.19
Cu	64	31	35	33	34	32	22	23	21	29	24	22	23	25	32	24	29.62
Zn	108	63	66	69	71	71	54	46	43	52	62	63	48	56	49	57	61.12
Ga	9	10	10	11	11	11	26	20	19	21	23	22	19	24	25	24	17.81
Pb	39	23	24	24	21	22	93	59	41	52	66	48	77	89	72	51	50.06
Th	14	15	13	13	15	12	14	14	16	15	14	16	15	15	15	14	14.37
Rb	73	74	81	83	87	86	116	95	105	99	106	96	109	138	107	103	97.37
U	1.9	1.6	2.1	2	3.8	2.1	2.2	2.1	2.4	2	2.1	1.9	2.1	2.3	2.1	1.8	2.16
Sr	40	37	41	66	61	63	75	64	73	75	79	64	65	80	68	72	63.94
Y	25	28	27	28	28	27	20	19	20	21	19	20	21	21	24	26	23.37
Zr	287	481	329	321	333	272	179	185	251	154	252	175	320	250	256	255	268.75
Nb	13	15	15	14	14	15	12	11	11	12	12	12	11	12	12	11	12.62

**Table 4** Estimated rare earth elements (REEs) concentration (in mg kg<sup>-1</sup>) for the Tawi River sediments

Sample no.	T-1	T-2	T-3	T-4	T-5	T-6	T-7	T-8	T-9	T-10	T-11	T-12	T-13	T-14	T-15	T-16	Avg
La	36.9	68.2	38.8	46.8	42.9	38.8	38.1	40.1	43.7	36.8	47.2	46.1	36.9	50.1	58.2	42.9	44.53
Ce	75.0	141.2	80.8	95.4	87.8	78.8	74.8	80	88.2	75.3	79.4	82.8	90.1	96.8	89.5	94.9	88.17
Pr	7.81	4.4	8.8	10	9.1	8.1	8.7	8.9	9.5	10.4	9.5	10.9	8.5	9.8	10.6	10.2	9.7
Nd	31.7	58.4	36.9	40.8	37.1	32.8	33.5	33.9	36.4	36.2	37.5	35.1	35.7	31.5	40.4	33.1	36.94
Sm	6.1	10.1	7.3	7.8	7.2	6.3	7.4	6.9	7.8	7.5	7.7	7.8	8.5	8.3	7.5	8.3	7.66
Eu	1.1	1.7	1.2	1.4	1.3	1.2	1.4	1.4	1.6	1.5	1	1.4	1.6	1	1.4	1.5	1.36
Gd	4.7	7.3	5.9	5.6	5	4.4	5.2	5.3	5.2	5	5.5	5.9	4.9	5.1	5.4	4.8	5.32
Tb	0.8	1.1	0.8	0.9	0.9	0.8	0.8	0.8	0.7	0.8	0.9	0.9	0.8	0.8	0.9	0.9	0.85
Dy	4.2	5.1	4.1	4.7	4.7	4.3	4.1	4	4.1	4.2	4.3	4.5	4.4	5	5.1	4.9	4.48
Ho	0.9	0.9	0.8	0.9	0.9	0.9	0.9	0.8	0.9	0.9	1	1	0.8	0.9	1	0.9	0.9
Er	2.6	2.8	2.3	2.8	2.7	2.5	2.1	1.9	2.1	2.3	2.9	2.9	2.6	2.5	3	2.9	2.56
Tm	0.4	0.4	0.3	0.4	0.4	0.4	0.3	0.3	0.4	0.3	0.3	0.3	0.4	0.3	0.3	0.3	0.34
Yb	2.2	2.3	2	2.3	2.4	2.2	1.9	1.8	1.9	1.9	1.8	2.2	1.9	2	2.2	1.9	2.01
Lu	0.3	0.3	0.3	0.3	0.4	0.3	0.3	0.2	0.3	0.4	0.3	0.4	0.3	0.2	0.3	0.3	0.31
Th/Sc	1.75	1.88	1.63	1.08	1.5	1.2	0.48	0.56	0.67	0.65	0.58	0.52	0.55	0.6	0.53	0.52	0.92
Zr/Sc	35.88	60.12	41.12	26.75	33.3	27.2	6.17	7.4	10.45	6.7	10.5	5.64	11.85	10	9.14	9.44	19.48
Eu/Eu*	0.6	0.58	0.54	0.62	0.63	0.66	0.66	0.68	0.72	0.71	0.48	0.61	0.7	0.44	0.64	0.69	0.62
Gd <sub>N</sub> /Yb <sub>N</sub>	1.73	2.57	2.39	1.97	1.69	1.62	2.21	2.38	2.21	2.12	2.47	2.17	2.09	2.06	1.98	2.04	2.14

### 5.1.2 Trace elements

The concentrations of trace elements of the Tawi River sediments show large variations (Table 3). In particular, Zr, Rb, Sr, Zn, Pb and Cu occur in appreciable amounts in these sediments (Table 3). Being highest among the trace elements, Zr content is greater than the upper continental crust (UCC, 193 mg kg<sup>-1</sup>; after Taylor & McLennan, 1985) and Post-Archean Australian Shale (PAAS, 210 mg kg<sup>-1</sup>; after Rudnick & Gao, 2014). The Ni concentration is less than the Cu ranging from 21 to 64 mg kg<sup>-1</sup>

with an average value 29.62 mg kg<sup>-1</sup>. The Sc shows an average value 19.93 mg kg<sup>-1</sup> and the Ga has an average value 17.81 mg kg<sup>-1</sup>. The Th ranging from 12 to 16 mg kg<sup>-1</sup> has an average value 14.37 mg kg<sup>-1</sup>. The U shows very little variation, and majority of the samples have its values between 2.0 and 2.4 mg kg<sup>-1</sup>, respectively.

### 5.1.3 Rare earth elements (REEs)

The concentrations of rare earth elements (REEs) of the Tawi River sediments show large variations (Table 4).

Total REE ( $\sum\text{REE}$ ) concentration of the Tawi River sediment ranges between  $174 \text{ mg kg}^{-1}$  and  $304 \text{ mg kg}^{-1}$ , averaging to  $204 \text{ mg kg}^{-1}$ . The average  $\sum\text{REE}$  data show a relatively higher value than the average value for the UCC ( $148 \text{ mg kg}^{-1}$ ; Rudnick & Gao, 2014). The  $\text{Eu}/\text{Eu}^*$  values vary from 0.44 to 0.72 with an average value of 0.62 and most of the sediment samples also show negative Eu anomalies. The average  $\text{Eu}/\text{Eu}^*$  (0.62) value of the sediments is very close to the average value of the UCC ( $\text{Eu}/\text{Eu}^*$ , 0.65; Rudnick & Gao, 2014). The  $\text{La}_N/\text{Yb}_N$  of the sediment samples range from 13.17 to 17.97 (avg. 15.04), which is relatively higher than the UCC value of 10.69 (Rudnick & Gao, 2014) and the PAAS value of 9.17 (Taylor & McLennan, 1985). The  $\text{Gd}_N/\text{Yb}_N$  of the sediment samples varying from 1.72 to 2.56 (avg. 2.14), are relatively higher than the UCC value of 1.65 (Rudnick & Gao, 2014) and the PAAS value of 1.36 (Taylor & McLennan, 1985).

## 6 Discussion

### 6.1 Bulk geochemical composition

Harker bivariate diagrams of the  $\text{Al}_2\text{O}_3$  versus major oxides show a correlation of varying strength in the sediment samples. In the present case with increasing in  $\text{Al}_2\text{O}_3$  content, the  $\text{SiO}_2$  subsequently decreases due to variable sediment sorting and hydrodynamic fractionation controlling its distribution.  $\text{Al}_2\text{O}_3$  shows a strong negative correlation with  $\text{SiO}_2$  ( $r^2 = -0.94$ ) and positive correlation with  $\text{Fe}_2\text{O}_3$  ( $r^2 = 0.72$ ),  $\text{K}_2\text{O}$  ( $r^2 = 0.83$ ),  $\text{MgO}$  ( $r^2 = 0.91$ ) and  $\text{TiO}_2$  ( $r^2 = 0.20$ ).

The increasing trend and positive correlation of other elements with  $\text{Al}_2\text{O}_3$  suggest the control of aluminous clay or heavy minerals in specific size grades (Hossain et al., 2017). The lack of significant correlation of  $\text{Al}_2\text{O}_3$  with  $\text{Na}_2\text{O}$  shows its conserved nature in all the studied samples (Fig. 2). Other oxides like  $\text{CaO}$ ,  $\text{MnO}$  and  $\text{P}_2\text{O}_5$ , which do not show any significant correlation with  $\text{Al}_2\text{O}_3$ , also suggest scattered distribution among all the studied samples.  $\text{CaO}$  concentration is low near the source; however, it slightly increases and maintains consistency throughout the river. The concentration and distribution of  $\text{CaO}$  and  $\text{Na}_2\text{O}$  is linked with relatively coarse size fraction of the sediments and abundance in low weathered fractions (Hossain, 2019; Hossain et al., 2018). Their  $\text{CaO}$  and  $\text{Na}_2\text{O}$  low concentrations are justified because of fine-grained nature of the studied sediments.

Elemental concentrations of sediments normalized relative to the average Upper Continental Crust (UCC) have been presented along with average Siwalik mudstone (see Sinha et al., 2007) and average Murree sandstone (see Singh et al., 1990) for the comparison (Fig. 3). Figure 3 shows that most of the major oxides in the Tawi sediments show mean

normalized values less than 1, that is lower than the UCC, implicating removal of mobile elements from the sediments during extensive weathering and erosion processes (e.g. Bastia et al., 2020; Hossain et al., 2017; Kanhaiya et al., 2018a, 2018b; Mondal et al., 2012).  $\text{SiO}_2$  having mean normalized value of more than 1 shows higher concentrations compared with UCC in the Tawi sediments. Enriched concentration of  $\text{SiO}_2$  and  $\text{SiO}_2/\text{Al}_2\text{O}_3$  ratio (ranging from 4.18 to 10.33, avg. 5.69) can be related to the presence of more quartz (e.g. Bastia et al., 2020; Potter, 1978). The slight depletion in all other oxides compared to UCC can be explained by their relatively more mobile nature during transportation of the Tawi sediments (e.g. Garzanti & Resentini, 2016; Mondal et al., 2012; Nesbitt & Young, 1982, 1984). A similar observational fact was observed in the case of the Siwalik mudstone and Murree sandstone. This can be justified by the similar mineral assemblage of the Siwalik mudstone and Tawi sediments which are rich in above oxides (Sinha et al., 2007). The Murree sandstone also shows more concentration of  $\text{SiO}_2$ ,  $\text{MgO}$ ,  $\text{MnO}$  and  $\text{Na}_2\text{O}$  than the Tawi sediments due to similarities in their mineralogical constituents (see Singh et al., 1990).

Among the trace elements, Ga, Rb and Ni show positive correlations with  $\text{Al}_2\text{O}_3$ , indicating their distribution and association with clay minerals. Also they are linked to variation in degree of sediment sorting of the river. The Ca and Zn show negative correlation with  $\text{Al}_2\text{O}_3$ . Trace elements like Th, Zr, U, Co, Pb, Y and Nb have no significant correlation with  $\text{Al}_2\text{O}_3$  (Fig. 4) suggesting their association with heavy minerals (e. g. Garzanti et al., 2010, 2011).

The enrichment of Zr, Th and Y than the UCC indicates that their abundances are primarily controlled by resistant heavy minerals like zircon, monazite and apatite (Garzanti et al., 2016; Hossain, 2019). Strontium (Sr) is showing depletion relative to the UCC, indicating disintegration of feldspar during prolonged chemical weathering. Enrichment of Rb compared to UCC is due to its association with K- feldspar, mica and clay minerals (e. g. Hossain, 2019; Kanhaiya et al., 2018a, 2018b; Mondal et al., 2012). Trace elements such as Pb and Y also show enrichment compared to the UCC suggesting alteration of clay minerals during weathering process (Fig. 5).

### 6.2 Textural and mineralogical maturity

Two major log ratios of  $\text{SiO}_2/\text{Al}_2\text{O}_3$  and  $\text{Na}_2\text{O}/\text{K}_2\text{O}$  (Pet-tijohn et al., 1972) and log ratios of  $\text{SiO}_2/\text{Al}_2\text{O}_3$  and  $\text{Fe}_2\text{O}_3/\text{K}_2\text{O}$  (Herron, 1988) have been used to classify Tawi sediments. Based on these two log ratios, the Tawi sediments have been categorized as arkose with subordinate amount of litharenite proportion (Fig. 6a, b). The above classification schemes, thus, suggest that the Tawi sediments are texturally and mineralogically immature in nature. The similar observational facts have been observed in case of other Himalayan

**Fig. 2** Selected major oxides–Al<sub>2</sub>O<sub>3</sub> variation plots for the Tawi River sediments showing compositional variations

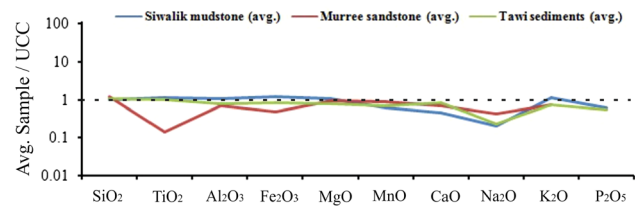
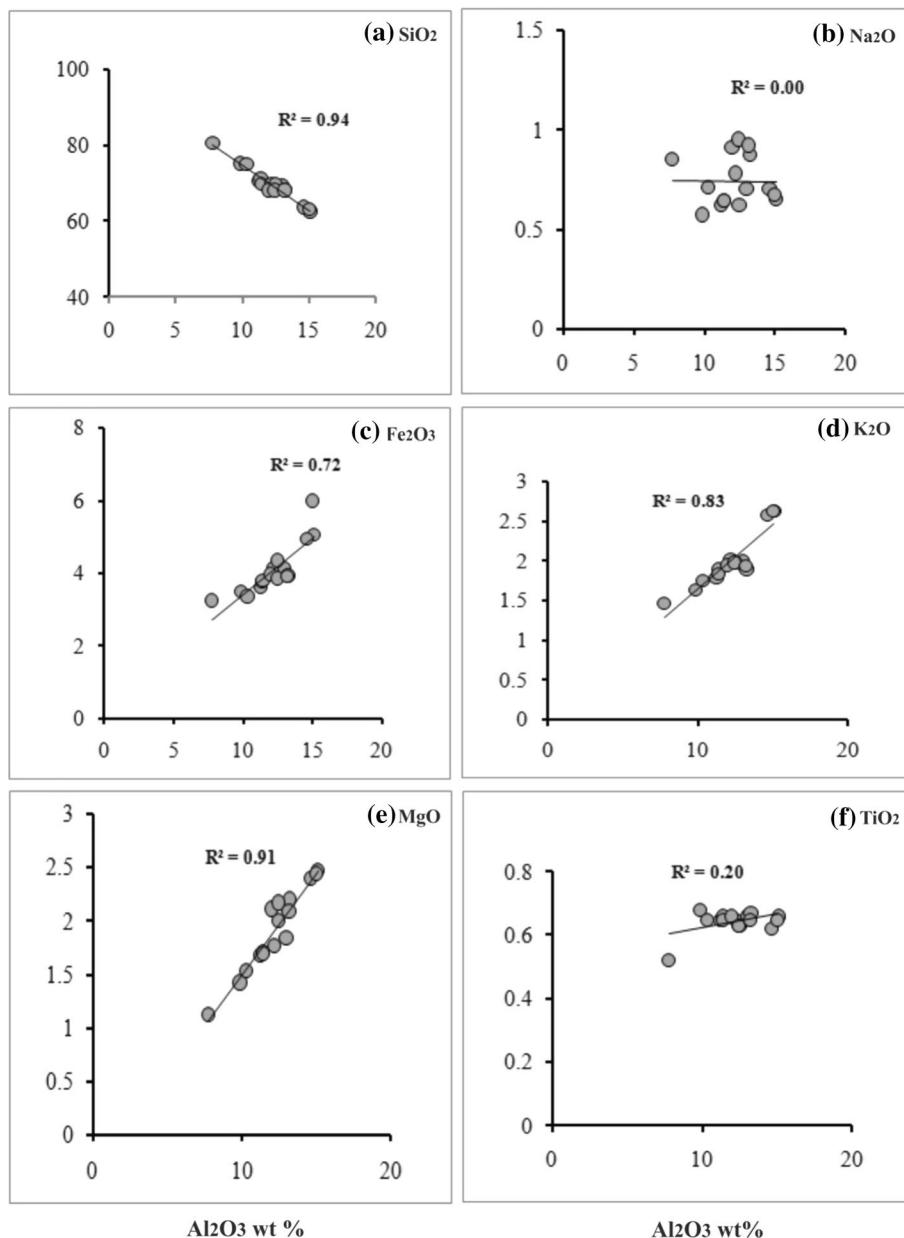


**Fig. 3** UCC (upper continental crust) normalized average major oxide compositions of the Tawi River sediments. The major oxide compositions of Siwalik mudstone (after Sinha et al. 2007) and Murree sandstone (after Singh et al., 1990) are shown for comparison

ivers, e.g., Hindon and Meghna (Hossain, 2019; Mondal et al., 2012).

The SiO<sub>2</sub>/Al<sub>2</sub>O<sub>3</sub> ratio is widely studied for implicating textural maturity and sorting of sediments (Ramos-Vazquez et al., 2017; Roser et al., 1996). In acidic and basic igneous rock average SiO<sub>2</sub>/Al<sub>2</sub>O<sub>3</sub> ratio comes out to be around 3 and 5, respectively (Roser et al., 1996), whereas average SiO<sub>2</sub>/Al<sub>2</sub>O<sub>3</sub> value in clastic sediments comes around 5 and indicates sediment maturity. The average SiO<sub>2</sub>/Al<sub>2</sub>O<sub>3</sub> value of the Tawi sediments is 5.69 suggesting low to moderate textural maturity.

The index of composition variability, ICV = (Fe<sub>2</sub>O<sub>3</sub> + K<sub>2</sub>O + Na<sub>2</sub>O + MgO + TiO<sub>2</sub>)/Al<sub>2</sub>O<sub>3</sub> (Cox et al., 1995) is widely used as a tool to evaluate the mineralogical maturity

**Fig. 4** Selected trace element– $\text{Al}_2\text{O}_3$  variation plots for the Tawi River sediments

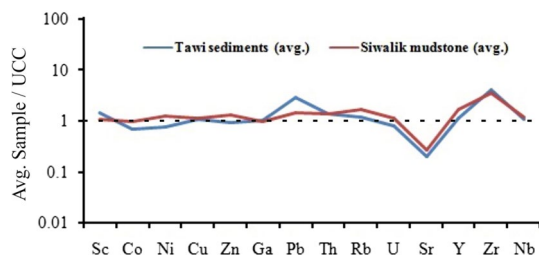
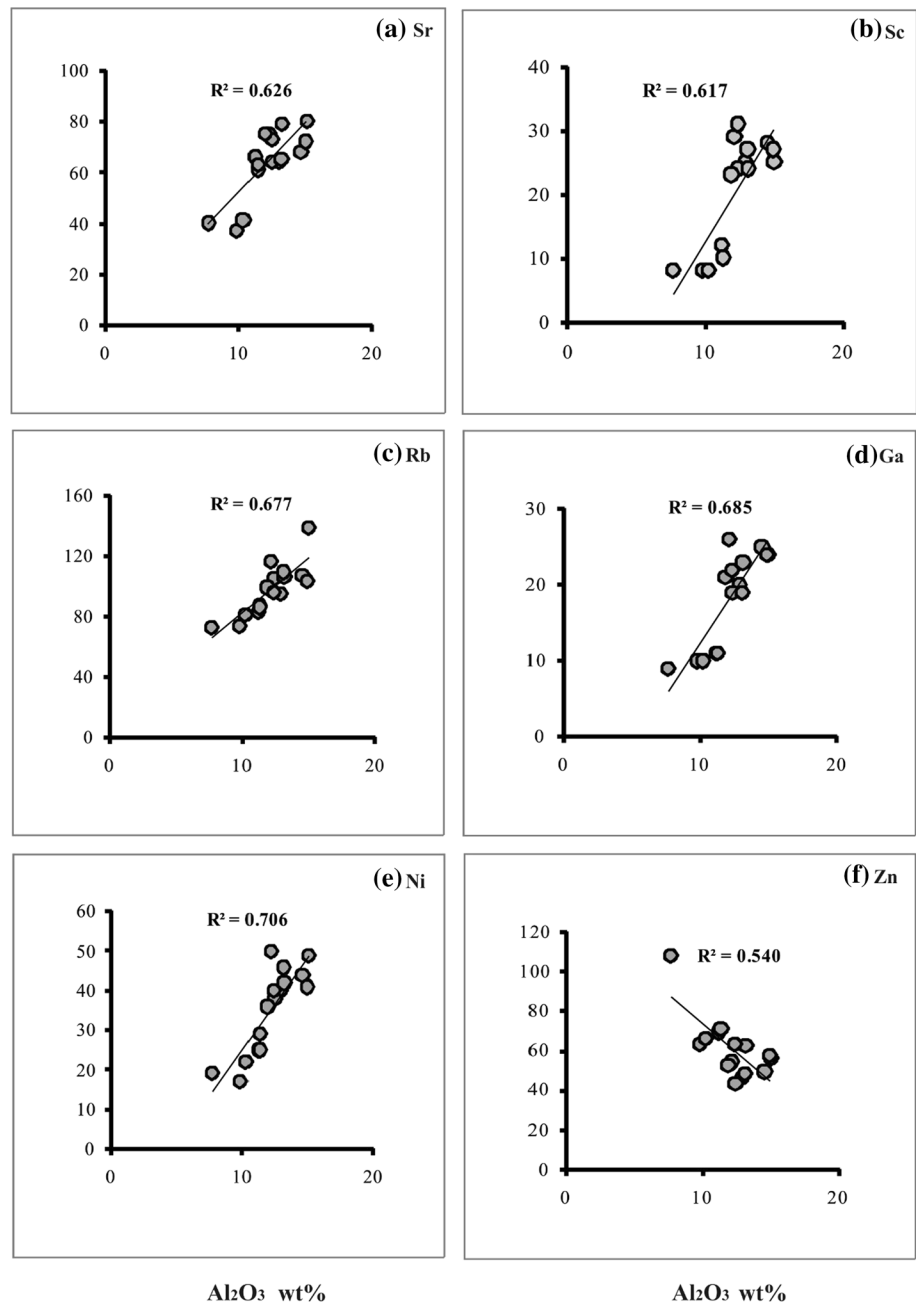


**Fig. 5** UCC (upper continental crust) normalized trace elements (average) compositions of the Tawi River sediments. The trace elements composition of Siwalik mudstone (after Sinha et al., 2007) is shown for comparison

of sediments. The ICV values for rock-forming minerals are higher ( $>0.84$ ), while clay minerals have lower ICV values ( $<0.84$ ) (Cox et al., 1995). The high ICV values in clastic sediments indicate textural immaturity, while low ICV values indicate recycling and/or a highly weathered source rock (Cox et al., 1995; Hossain et al., 2018). The Tawi sediments exhibit high ICV values ranging from 0.88 to 1.16 (avg. 1.01) and are within the range of typical UCC (upper continental crust) and PAAS (Post-Archean Australian Shale) (Taylor & McLennan, 1985; Fig. 7), implying that they are likely concomitant with major rock forming minerals which are mineralogically immature in nature.



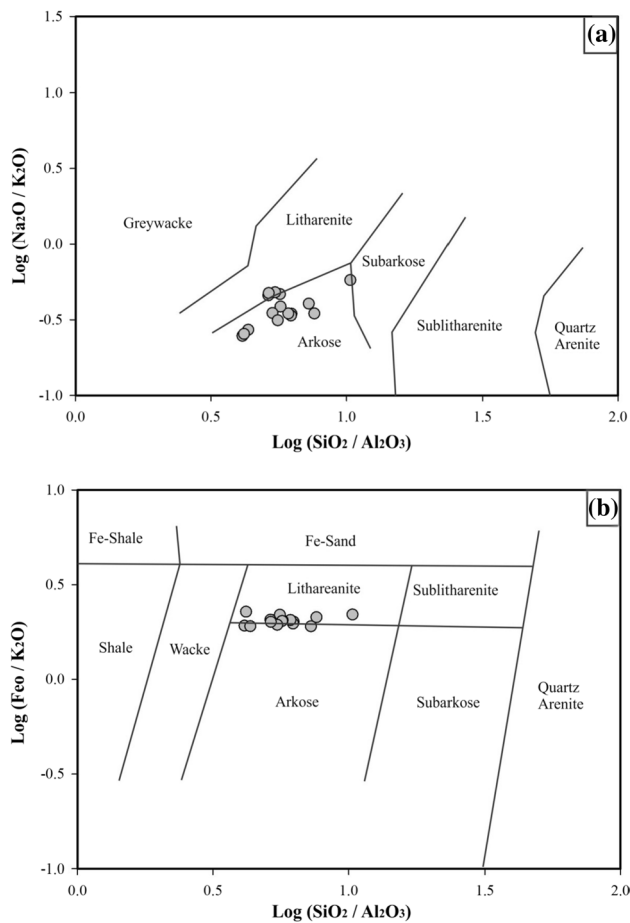


**Fig. 6** a  $\text{Log Na}_2\text{O}/\text{K}_2\text{O}$ – $\text{Log SiO}_2/\text{Al}_2\text{O}_3$  (after Pettijohn et al., 1972), b  $\text{Log FeO}/\text{K}_2\text{O}$ – $\text{Log SiO}_2/\text{Al}_2\text{O}_3$  (Herron, 1988) relationship patterns for the studied Tawi River sediments

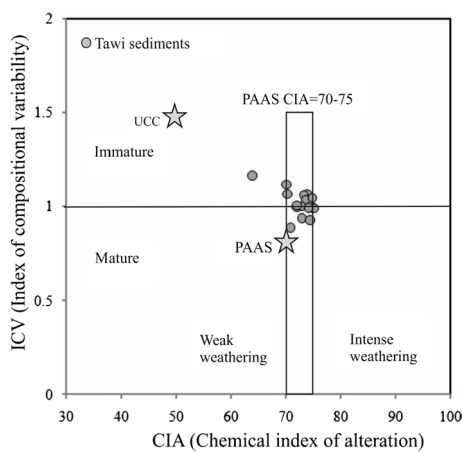


**Fig. 7** Index of compositional variability (ICV) versus Chemical index of alteration (CIA) plot (after Long et al., 2012) for the Tawi River sediments. The upper continental crust (UCC) and Post-Archean Australian Shale (PAAS) values are taken from Taylor and McLennan (1985)

### 6.3 Palaeoweathering

Chemical weathering of rocks is observed to have a huge influence on global climate as it affects the atmospheric  $\text{CO}_2$  concentration (Berner, 1992, 1995; Dupre et al., 2003). Convergence of Indian and Asian plates during Cenozoic period led to the tectonic uplift of the Himalaya that influenced the Himalayan foreland and modern Himalayan rivers and its tributaries in terms of climate (precipitation) and ocean water chemistry in and around Indian Subcontinent (Singh & Lee, 2007). To quantitatively measure the degree of weathering, Nesbitt and Young (1982, 1984) defined a chemical index of alteration i.e.,  $\text{CIA} = [\text{Al}_2\text{O}_3 / (\text{Al}_2\text{O}_3 + \text{CaO}^* + \text{Na}_2\text{O} + \text{K}_2\text{O})] \times 100$ , where  $\text{CaO}^*$  denotes Ca in the silicate phases only. The CIA value for freshly exposed rock is 50 and for average shale CIA values vary from 70 to 75, which reflect the presence of weathering products like muscovite, illite and smectite. Intensely weathered rocks have CIA values approaching 100 (Fedo et al., 1995; Nesbitt & Young, 1982, 1984) and composition close to kaolinite or gibbsite. The CIA values of the Tawi sediments varying from 63.9 to 75.2 with an average value of 72.6, suggesting moderate intensity of chemical weathering in the source areas.

The CIA values are also graphically represented in the  $\text{Al}_2\text{O}_3$ – $(\text{CaO}^* + \text{Na}_2\text{O})$ – $\text{K}_2\text{O}$  (A–CN–K) triangular plot (Fig. 8a) to investigate weathering trends and bulk source composition, as well as the extent of post depositional K-metasomatism (Fedo et al., 1995; Kanhaiya et al., 2018a, 2018b; Nesbitt & Young, 1984). The Tawi sediments show a loss in  $\text{K}_2\text{O}$ ,  $\text{Na}_2\text{O}$ , and  $\text{CaO}$ , when compared to UCC on the A–CN–K plot (Fig. 8a), and follow the ideal weathering trend. The K-corrected CIA in the sediments (avg. 72.6) is indicative of moderate intensity of chemical weathering in the Tawi River catchment area also supported by the comparable data from other Himalayan rivers and marine sediments (Hossain et al., 2017; Lupker et al., 2012; Mondal et al., 2012).

The chemical index of alteration (CIA) values is consistent with plagioclase index of alteration (PIA) (Fedo et al., 1995). The  $\text{PIA} = [(\text{Al}_2\text{O}_3 - \text{K}_2\text{O}) / (\text{Al}_2\text{O}_3 + \text{CaO}^* + \text{Na}_2\text{O} - \text{K}_2\text{O})] \times 100$ , where  $\text{CaO}^*$  represents Ca in the silicate phases only (Fedo et al., 1995). The PIA values for the Tawi sediments ranging from 69.2 to 85.7 (avg., 80.9) indicate alteration of feldspars and moderate chemical weathering environment in the river catchment.

The PIA values are plotted graphically in the  $(\text{Al}_2\text{O}_3 - \text{K}_2\text{O})$ – $\text{CaO}^*$ – $\text{Na}_2\text{O}$  (A–C–N) ternary plot (Fig. 8b) and reflect the weathering trends and alteration of plagioclase feldspars. The (A–C–N) ternary diagram (Fig. 8b) shows relatively high values of PIA in the Tawi sediments indicating moderate degree of plagioclase weathering. In the (A–C–N) triangular plot, all the samples are

**Fig. 8** Ternary plots of the studied Tawi River sediments. **a** Major elements compositions plotted as molar proportion on an  $\text{Al}_2\text{O}_3$ – $(\text{CaO} + \text{Na}_2\text{O})$ – $\text{K}_2\text{O}$  (A–CN–K) diagram (arrow indicates the weathering trend of the sediments, the scale showing the chemical index of alteration (CIA) is shown at the right side), **b** major element compositions of sediments plotted as molar proportions on an  $(\text{Al}_2\text{O}_3 - \text{K}_2\text{O})$ – $(\text{CaO})$ – $\text{Na}_2\text{O}$  (A–C–N) diagram (the scale showing the plagioclase index of alteration (PIA) is shown at the right side), **c** major element compositions of sediments plotted as molar proportions on an  $\text{Al}_2\text{O}_3$ – $(\text{CaO} + \text{Na}_2\text{O} + \text{K}_2\text{O})$ – $(\text{Fe}_2\text{O}_3 + \text{MgO})$  (A–CNK–FM) diagram. The upper continental crust (UCC) and Post-Archean Australian shale (PAAS) (after Taylor & McLennan, 1985), Siwalik mudstone (after Sinha et al., 2007) and Murree sandstone (after Singh et al., 1990) are shown for comparison

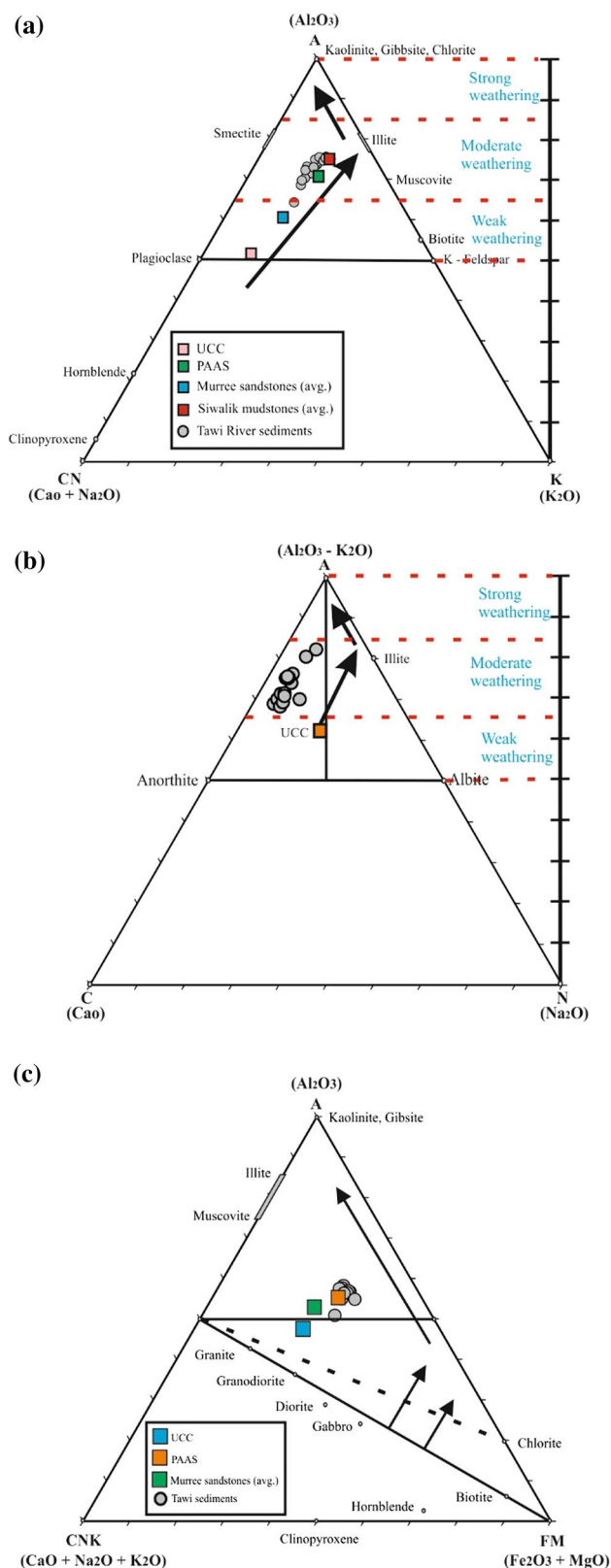
showing distribution field near the A apex which can be related to the effect of substantial weathering.

The CIA is the resultant value of measuring proportion of  $\text{Al}_2\text{O}_3$  versus labile oxides. High CIA value means removal of labile cations like  $\text{Ca}^{2+}$ ,  $\text{Na}^{2+}$  and  $\text{K}^{1+}$  compared to stable cations like  $\text{Al}^{3+}$ ,  $\text{Ti}^{2+}$  during the course of weathering. Hence, aluminium-rich clay minerals have higher CIA values and primary minerals have lower CIA values. The negligible variation in CIA and PIA values of the Tawi sediments can be reflective of textural and compositional homogeneity leading to no larger variations in major element concentration.

The CIA and PIA values (Nesbitt & Young, 1982) are useful to evaluate the degree of the chemical weathering to which the sedimentary rocks are subjected consequently affecting mineral geochemistry of sediments. High CIA values are suggestive of hot and humid climate whereas low CIA values suggest almost negligible chemical alteration and consequently reflect cool and/or arid conditions (Fedo et al., 1995; Nesbitt & Young, 1982). The moderate CIA and PIA values suggest moderate weathering intensity in the Tawi River catchment. The major part of Tawi catchment experiences a subtropical monsoonal climate, which may be responsible for moderate weathering intensity.

Intensity of weathering in the Tawi sediments can also be assessed from the A–CNK–FM i.e.,  $(\text{Al}_2\text{O}_3)$ – $(\text{CaO}^* + \text{Na}_2\text{O} + \text{K}_2\text{O})$ – $(\text{Fe}_2\text{O}_3 + \text{MgO})$  triangle plot proposed by Nesbitt and Young (1989). All of the sediments in this plot have distributions that are similar to the average composition of granite, granodiorite, and diorite, as well as the UCC, implying a usual felsic to intermediate source composition. All of the sediments have a distribution that is extremely similar to PAAS and Murree sandstones as well as Siwalik mudstones (Singh et al., 1990; Sinha et al., 2007). All of the values in the investigated sediments are above the feldspar–smectite tie line and heading towards the A ( $\text{Al}_2\text{O}_3$ )–apex indicating dominance of feldspar and enrichment of kaolinite during progressive weathering (Fig. 8c).

The elemental ratios Rb/Sr and  $\text{K}_2\text{O}/\text{Rb}$  ratios in UCC are 0.32 and 252, respectively (Taylor & McLennan, 1985). The



Rb/Sr ratios varying from 1.2 to 2.0 (avg. 1.5) are more than the UCC and  $\text{K}_2\text{O}/\text{Rb}$  ratios ranging from 174.1 to 255.3 (avg. 205.4) are close to the UCC in the studied sediments.

These ratios also confirm the moderate to strong chemical weathering in the examined sediments where high Rb/Sr ratios ( $> 1$ ) in the sediments imply strong chemical weathering conditions and  $K_2O/Rb$  ratios  $< 250$  indicate moderate weathering (e.g. McLennan et al., 1993; Hossain et al., 2017).

#### 6.4 Provenance

Sediment geochemistry is a useful indicator of provenance as some trace elements and REEs have low or limited mobility during fluvial processes (McLennan et al., 1993; Roser & Korsch, 1988; Taylor & McLennan, 1985). Roser and Korsch (1988) categorized sandstone and argillite from several New Zealand greywacke terrains into four provenance groups, namely mafic (P1), intermediate (P2), felsic (P3) and recycled (P4), based on the abundance of seven major oxides. On the discriminate function plot (Fig. 9), majority of the Tawi sediment samples fall well within the felsic field (P3), suggesting felsic source rock provenance and progressive weathering environment.

The two oxides in the fluvial system that become less fractionated through weathering, transportation and diagenesis are  $Al_2O_3$  and  $TiO_2$  (Armstrong-Altrin et al., 2015; Rollinson, 1993). In determining the composition of mafic, intermediate and felsic source rocks, the  $Al_2O_3/TiO_2$  ratio is frequently used. The  $Al_2O_3/TiO_2$  ratio in mafic, intermediate, and felsic igneous rocks ranges from 3 to 8, 8 to 21, and 21 to 70, respectively (Hayashi et al., 1997). Here, most of the investigated samples have  $Al_2O_3/TiO_2$  ratios ranging from 14.5 to 23.9 (avg. 19.06), as well as high  $SiO_2$  contents (up to 80.30 wt%) suggesting that the Tawi sediments were largely generated from felsic source rock with some intermediate rock proportions.

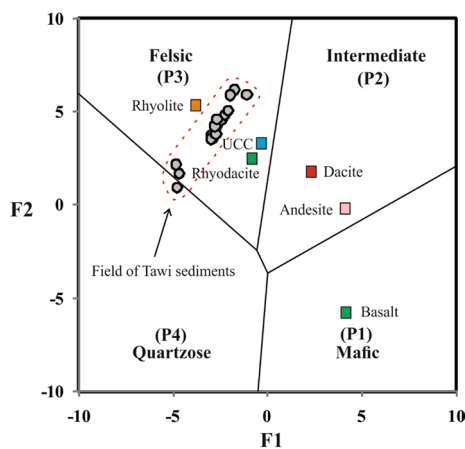


**Fig. 9** Major element provenance discriminant plot (after Roser & Korsch, 1988) of the studied Tawi River sediments indicating felsic nature

Following Floyd et al. (1989), the Ni versus  $TiO_2$  binary plot has been prepared, which also suggests the felsic nature of source rock from which the Tawi sediments have been derived (Fig. 10a). The Zr/Co versus Th/Co (McLennan et al., 1993) and Th/Yb versus La/Th (McLennan et al., 1980) are very useful bivariate plots in differentiating felsic and mafic source rocks. In these plots, all the studied samples show relatively high Th/Co and La/Th ratios indicating felsic provenance (Fig. 10b, c). As per Crook (1974), the  $Na_2O$  versus  $K_2O$  scatter diagram of the studied samples suggests that the Tawi sediments are rich in quartz (Fig. 11a). The examined sediments fall into the felsic provenance field in the Zr versus  $TiO_2$  bivariate plot of Hayashi et al. (1997), which divides source rocks into the following three divisions: mafic, intermediate, and felsic rocks (Fig. 11b). The greater Rb and  $K_2O$  contents as well as the K/Rb ratio below 230 (typical differentiated magmatic suite) indicate that

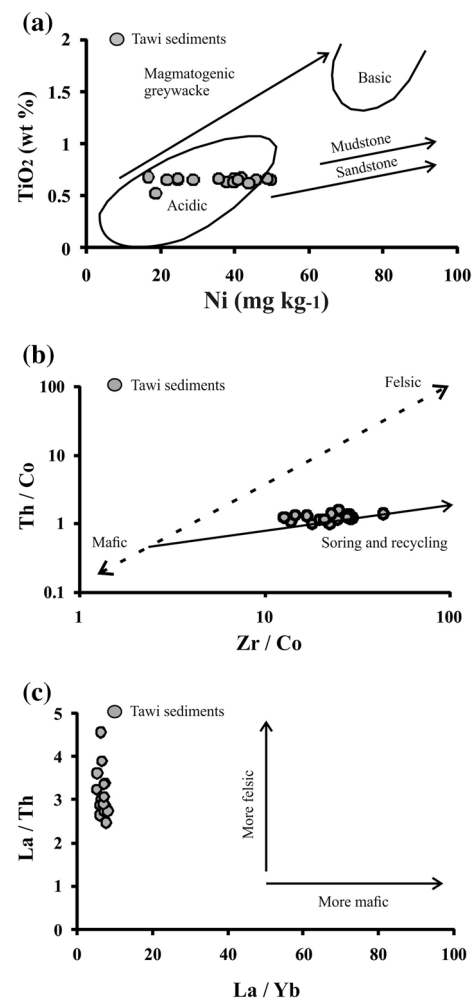


**Fig. 10** The bivariate plots **a** Ni– $TiO_2$  (after Floyd et al., 1989), **b** Zr/Co–Th/Co (after McLennan et al., 1993) and **c** Th/Yb–La/Th (after McLennan et al., 1980) showing the source rock characteristics of the Tawi River sediments

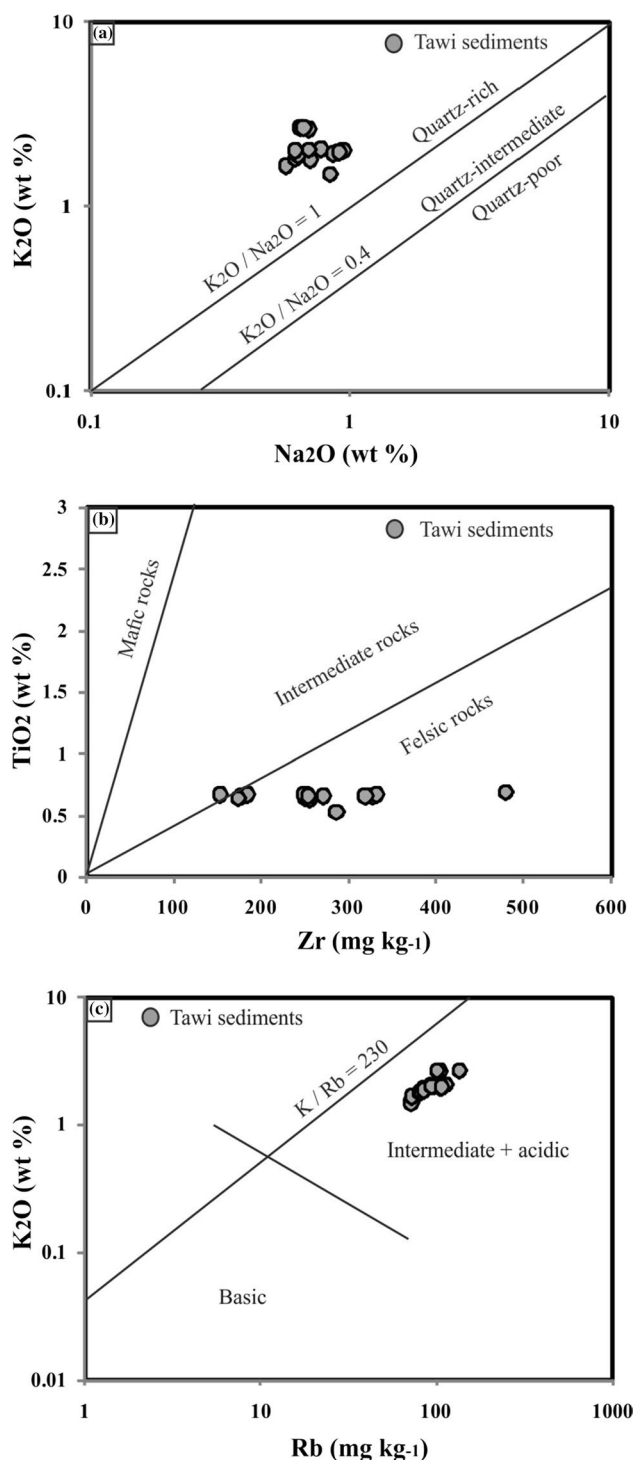


**Fig. 11** The bivariate plots of **a**  $\text{Na}_2\text{O}$ – $\text{K}_2\text{O}$  (after Crook, 1974), **b**  $\text{Zr}$ – $\text{TiO}_2$  (after Hayashi et al., 1997) and **c**  $\text{Rb}$ – $\text{K}_2\text{O}$  (after Shaw, 1968) showing the nature of source rock of the Tawi River sediments

these sediments are chemically coherent and derived mostly from acidic to intermediate source rocks (e. g. Shaw, 1968; Fig. 11c). In comparison to K, felsic rock weathering results in Rb enrichment due to distinct adsorption mechanisms and

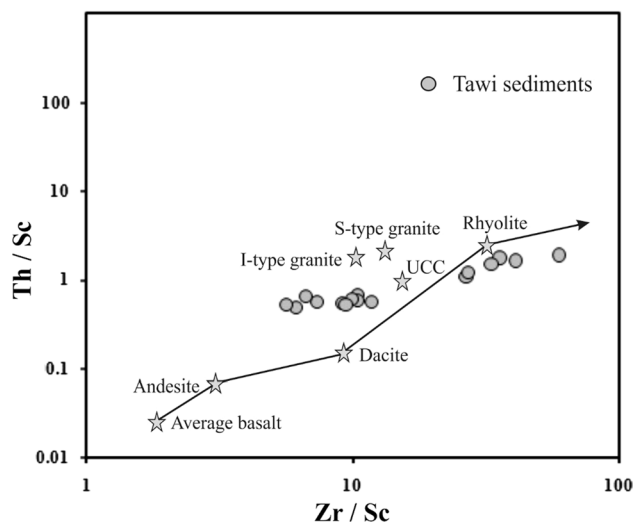


**Fig. 12** The  $\text{Th}/\text{Sc}$ – $\text{Zr}/\text{Sc}$  binary plot (after McLennan et al., 1993) of the Tawi River sediments

ion exchange (Heier & Billings, 1970). The low mobility of Rb has been found throughout the weathering processes due to its substantial sorption by clay minerals in the studied sediments (e. g. Dypvik & Harris, 2001).

On the  $\text{Th}/\text{Sc}$  versus  $\text{Zr}/\text{Sc}$  binary plot, the investigated sediments are scattered on both sides of the primary compositional trend (PCT) and closer to the average rhyolite, UCC, and I and S-type granites composition (e.g. McLennan et al., 1993; Fig. 12). The scattered distribution of sandy sediments associated with greater  $\text{Th}/\text{Sc}$  and  $\text{Zr}/\text{Sc}$  ratios implies loss of Sc and enrichment of zircon concentration due to hydraulic sorting or possible influence from recycled sediments sources.

The REE distributions and Eu anomalies are commonly utilised to distinguish mafic and felsic source compositions of the sediments (McLennan et al., 1993). The REE contents in the Tawi River sediments are enriched, averaging around  $204.5 \text{ mg kg}^{-1}$ , compared to an average UCC value of  $148 \text{ mg kg}^{-1}$  (Rudnick & Gao, 2014), implying that hydraulic fractionation may increase REE concentrations. In the Tawi sediments chondrite-normalized REE patterns show significant LREE enrichment, more or less flat HREE fractionation, and strong negative Eu anomalies (Fig. 13), which closely matches the range of typical granodiorite (Condie, 1993), UCC (Rudnick & Gao, 2014), and PAAS (Rudnick & Gao, 2014). The above observation shows that the sediments under investigation are primarily felsic in composition. The mafic igneous rocks display a less fractionated chondrite-normalized REE pattern with low  $\text{La}_N/\text{Yb}_N$  ratio values and no Eu anomalies (McLennan et al., 1993). The felsic igneous rocks, on the other hand, exhibit a highly fractionated chondrite-normalised REE pattern with high  $\text{La}_N/\text{Yb}_N$  ratios and large negative Eu anomalies (Taylor & McLennan, 1985).

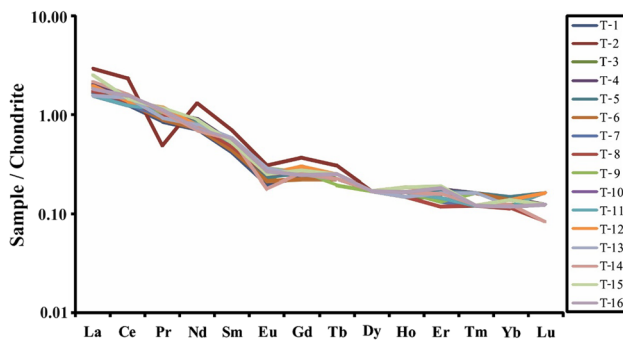


**Fig. 13** The chondrite-normalized REE pattern of the studied Tawi River sediments

The  $La_N/Yb_N$  ratios in the Tawi sediments range from 11.39 to 20.14 (avg. 15.04) (Table 4), which are quite near to normal Phanerozoic tonalite-trondhjemite-granodiorite (TTG; 8.9), granite (7.6; Condie, 1993), and UCC (10.96; Rudnick & Gao, 2014), implying a felsic provenance. On the other hand,  $La_N/Sm_N$  values in the studied samples ranging from 2.7 to 4.8 (avg. 3.6) are equivalent to the average UCC (4.15; Rudnick & Gao, 2014) and indicate that the sediments are derived from felsic upper crustal source. The variations in  $Eu/Eu^* - Gd_N/Yb_N$  have also been used to distinguish terrigenous sediment sources for a long time (McLennan, 1989). Most upper crustal rocks had  $Gd_N/Yb_N$  ratios of 1.0 to 2.0. (McLennan, 1989; McLennan et al., 1993). In the Tawi sediments, the  $Eu/Eu^*$  and  $Gd_N/Yb_N$  ratios range from 0.48 to 0.72 (avg. 0.62) and 1.62 to 2.57 (avg. 2.14) respectively indicating upper crustal (UCC) and andesitic composition (Fig. 14). The sediments also have a composition that falls between ordinary felsic volcanic rock (Condie, 1993) and UCC (Rudnick & Gao, 2014), indicating a felsic provenance.

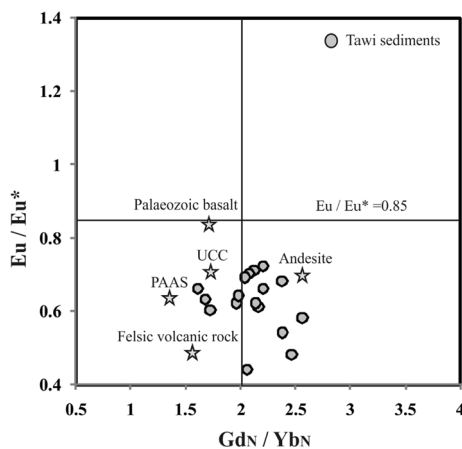


**Fig. 14** The  $Eu/Eu^* - Gd_N/Yb_N$  variation diagram (after McLennan, 1989) used to differentiate sources of the studied Tawi River sediments

In general the felsic igneous rock shows higher LREE/HREE ratios with strong negative Eu anomalies, whereas mafic igneous rock has lower LRRE/HREE ratios with low Eu anomalies. The LREE/HREE ratio for the Tawi sediments ranges from 14.71 to 23.11 (avg. 17.23), which is more or less close to the average UCC (8.68; Rudnick & Gao, 2014), and shows significant negative Eu anomalies (avg.  $Eu/Eu^*$ , 0.62), implying that the investigated sediments were primarily derived from felsic source rocks.

The extent to which the Tawi sediments keep the source properties was investigated using a bivariate plot of immobile element ratios such as  $Al_2O_3/SiO_2$  versus  $Fe_2O_3/SiO_2$  (Galy & France-Lonard, 2001). In addition to the Tawi sediments, we also plotted the available data from the Siwalik Sedimentary rocks, Lesser Himalaya, Higher Himalaya, and Trans-Himalayan Batholiths on this diagram for comparison (Fig. 15) (Galy & France-Lonard, 2001). The examined sediments are generally found in the fields of the Higher Himalaya, Lesser Himalaya, and Siwalik (Fig. 15), indicating that the Tawi sediments have retained the characteristics of the source rock from which they were derived.

## 6.5 Tectonics and climate

The geochemistry of detrital sediments is also extensively used to decipher the tectonic setting of sedimentary basin (Bhatia, 1983; Bhatia & Crook, 1986; Roser & Korsch, 1986). Roser and Korsch (1986) proposed a tectonic setting discrimination diagram based on  $K_2O/Na_2O$  and  $SiO_2$  binary plot that categorized sedimentary rocks into three tectonic settings viz. volcanic island arc (ARC), active continental margin (ACM), and passive margin (PM). On the diagram of Roser and Korsch (1986), the Tawi River sediments fall entirely in passive margin (PM) field (Fig. 16a). The  $K_2O/$

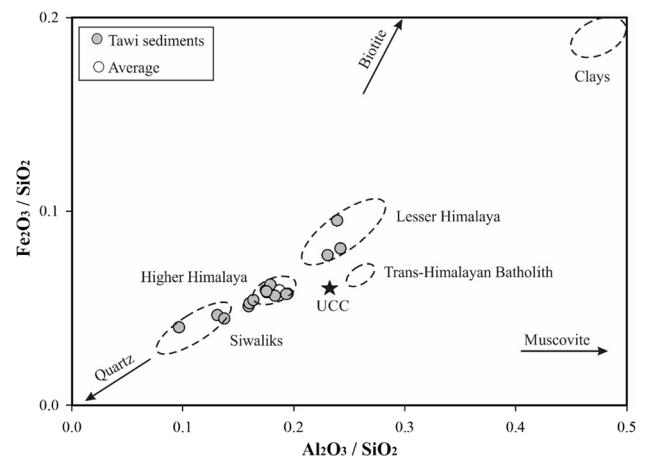


**Fig. 15** The  $Al_2O_3/SiO_2 - Fe_2O_3/SiO_2$  bivariate diagram for the Himalayan source rocks (after Galy & France-Lonard, 2001; Mondal et al., 2012)



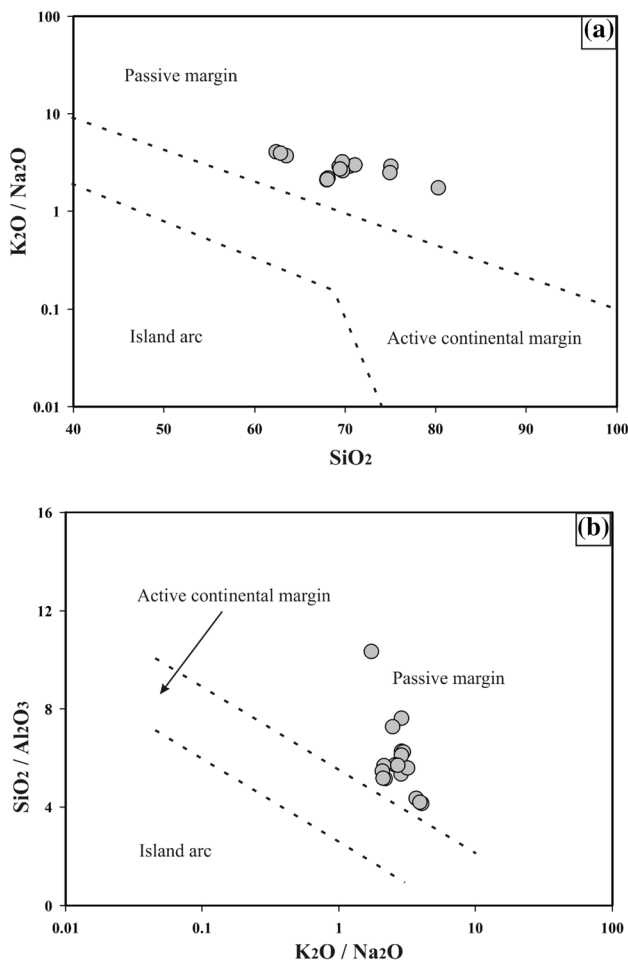


**Fig. 16** The tectonic setting discrimination diagrams **a**  $K_2O/Na_2O$ – $SiO_2$  binary plot (after Roser & Korsch, 1986), **b**  $K_2O/Al_2O_3$ – $SiO_2/Al_2O_3$  binary plot (after Maynard et al., 1982) showing passive margin tectonic setting for the Tawi River sediments

$Al_2O_3$  versus  $SiO_2/Al_2O_3$  bivariate plot given by Maynard et al. (1982) also suggests passive margin (PM) field for the Tawi River sediments (Fig. 16b). Sediments from plate interiors or stable continental zones are quartz-rich and low in feldspar, and they are plotted on the PM field (Roser & Korsch, 1986). Passive margin (PM) setting was also reported for Siwalik mudstones by Sinha et al. (2007). The active margin is made up of sediments from arc and collision settings, whereas the passive margin is made up of sediments from rift setting (Verma & Armstrong-Altrin, 2013). The passive margin field encompasses all Tawi sediments, inferring rift settings. A foreland basin, which comprises sediments produced from metasediments and recycled sedimentary rocks, does not belong to a rift setting. Singh (2013) suggested that the geochemical signatures of the sediments deposited in the foreland basins are either the passive margin sediments or between the active and passive continental margin sediments, while studying the Murree sedimentary

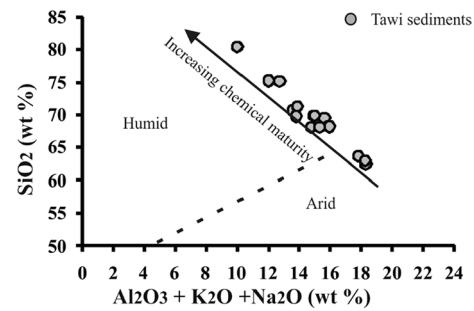


**Fig. 17** The bivariate plot of  $(Al_2O_3 + K_2O + Na_2O)$ – $SiO_2$  introduced by Suttner and Dutta (1986) is utilized to reveal the climate conditions in the catchment area of the Tawi River of the western Himalayan foreland, India

rocks. The two lithologies (Murree and Siwalik sandstones) contribute sediments chiefly to the Tawi River, which is a foreland basin without any doubt.

Suttner and Dutta (1986) have given a bivariate plot of  $(Al_2O_3 + K_2O + Na_2O)$  versus  $SiO_2$  to deduce the climate conditions in the catchment area of the Tawi River during sediment weathering and erosion. The majority of Tawi sediment samples fall in humid climate field (Fig. 17). This is also owing to the fact that the majority of the samples are immature in nature and have only been moderately weathered. Three samples clustered in the dry climatic field showed a lower degree of weathering, which could be attributed to the varied amounts of mean annual precipitation in different regions of the basin throughout the time.

## 7 Conclusions

Geochemical composition (major, trace and rare earth elements) of the Tawi River sediments have been studied to evaluate sediment type, compositional maturity, weathering intensity, provenance and tectonics. The key findings are as follows:

The Tawi River sediments are mostly arkosic in nature with a few litharenite fractions and have low compositional as well as mineralogical maturity. High concentration of  $SiO_2$  in Tawi sediments shows strong correlation with  $Al_2O_3$  representing progressive weathering and/or sorting effects.

The CIA, PIA, Rb/Sr and  $K_2O/Rb$  ratios and their relations in the sediments suggest moderate chemical weathering intensities. A–CN–K, A–C–N and A–CNK–FM plots also suggest moderate degree of chemical weathering under humid climatic conditions and the dominance of felsic provenance. Depletion of common labile elements ( $Na_2O$ , CaO,  $K_2O$ , Ba, and Sr) relative to UCC (upper continental crust) indicates loss of feldspar during the phase of chemical weathering in the source rock or during transportation in the fluvial regime.

The Zr and Th concentrations are considerably enriched in the Tawi River sediments as compared to UCC, signifying the occurrence of resistant heavy minerals, such as zircon in the source rocks.

The major elements discrimination diagram and immobile trace element ratios suggest that the Tawi River sediments were produced typically from felsic sources with compositions more or less similar to average rhyolite, granodiorite, UCC, and I- and S-type granites.

The chondrite-normalized REE patterns show LREE enrichment and nearly flat HREE pattern with significant negative Eu anomalies, pointing to felsic provenance again (mainly derived from Higher Himalaya). From the examined sediments, the tectonic setting signatures lead to a foreland basin or a passive continental margin setting.

**Acknowledgements** Authors are grateful to the Heads of their respective institutions for continuous support and encouragement. The Directors, WIHG, Dehradun and NGRI, Hyderabad are thankfully acknowledged for providing analytical facilities. S. Kanhaiya acknowledges the financial assistance from university grant commission (UGC), New Delhi vide Letter No. F. 30-517/2020 (BSR).

**Author contributions** MV and BPS have carried out the field work and processed the primary data. SK and SS drafted the first outline of the manuscript. All authors read and approved the final manuscript.

**Funding** The financial aid for the current work has been provided by the University grant commission (UGC), New Delhi vide Letter No. F. 30-517/2020 (BSR).

**Data availability statement** All the data are given in tabular form in the manuscript file.

## Declarations

**Conflict of interest** The authors declare that they have no competing interests.

## References

- Ahmad, F., Quasim, M. A., Absar, N., & Ahmad, A. H. M. (2022). Petrography and geochemistry of the Middle Jurassic Fort Member Sandstone, Jaisalmer Formation, Western India: Implications for weathering, provenance, and tectonic setting. *Geological Journal*, 1, 1–87. <https://doi.org/10.1002/gj.4372>.
- Armstrong-Altrin, J. S., Machain-Castillo, M. L., Rosales-Hoz, L., Carranza-Edwards, A., Sanchez-Cabeza, J. A., & Ruiz-Fernández, A. C. (2015). Provenance and depositional history of continental slope sediments in the South western Gulf of Mexico unravelled by geochemical analysis. *Continental and Shelf Research*, 95, 15–26. <https://doi.org/10.1016/j.csr.2015.01.003>.
- Babeesh, C., Lone, A., & Achyuthan, H. (2017). Geochemistry of Mensal lake sediments, Kashmir: Weathering, provenance and tectonic setting. *Journal of Geological Society of India*, 89(5), 563–572.
- Bastia, F., Equeenuddin, S. M., Roy, P. D., & Hernández-Mendiola, E. (2020). Geochemical signatures of surface sediments from the Mahanadi river basin (India): Chemical weathering, provenance, and tectonic settings. *Geological Journal*. <https://doi.org/10.1002/gj.3746>.
- Berner, R. A. (1992). Weathering, plants, and the long term carbon cycle. *Geochimica Et Cosmochimica Acta*, 56, 3225–3231.
- Berner, R. A. (1995). Chemical weathering and its effect on atmospheric CO<sub>2</sub> and climate. In A. F. White & S. L. Brantley (Eds.), *Chemical weathering rates of silicate minerals* (Vol. 31, pp. 565–583). Chantilly: Mineralogical Society of America.
- Bhatia, M. R. (1983). Plate tectonics and geochemical composition of sandstones. *Journal of Geology*, 91, 611–627. <https://doi.org/10.1086/628815>.
- Bhatia, M. R., & Crook, K. A. (1986). Trace element characteristics of graywackes and tectonic setting discrimination of sedimentary basins. *Contributions to Mineralogy and Petrology*, 92, 181–193. <https://doi.org/10.1007/BF00375292>.
- Condie, K. C. (1993). Chemical composition and evolution of the upper continental crust: Contrasting results from surface samples and shales. *Chemical Geology*, 104, 1–37. [https://doi.org/10.1016/0009-2541\(93\)90140-E](https://doi.org/10.1016/0009-2541(93)90140-E).
- Condie, K. C., Dengate, J., & Cullers, R. L. (1995). Behaviour of rare earth elements in a palaeoweathering profile on granodiorite in the Front Range, Colorado, U.S.A. *Geochimica Et Cosmochimica Acta*, 59, 279–274.
- Cox, R., Lowe, D. R., & Cullers, R. L. (1995). The influence of sediment recycling and basement composition on evolution of mud rock chemistry in the south western United States. *Geochimica Et Cosmochimica Acta*, 59, 2919–2940. [https://doi.org/10.1016/0016-7037\(95\)00185-9](https://doi.org/10.1016/0016-7037(95)00185-9).
- Crook, K. A. (1974). Lithogenesis and geotectonics: the significance of compositional variation in flysch arenites (Graywackes). In R. H. Dott & R. H. Shaver (Eds.), *Modern and ancient geosynclinal sedimentation* (Vol. 19, pp. 304–310). Tulsa: Society for Sedimentary Geology (SEPM) Special Publication.
- Das, A., & Krishnaswami, S. (2007). Element geochemistry of river sediments from the Deccan Traps, India: Implications to sources of elements and their mobility during basalt-water interaction. *Chemical Geology*, 242, 232–254.
- Derry, L. A., & France-Lanord, C. (1996). Neogene Himalayan weathering history and river <sup>87</sup>Sr/<sup>86</sup>Sr: impact on marine Sr record. *Earth and Planetary Science Letters*, 142, 59–74.
- Drever, J. I., & Zobrist, J. (1992). Chemical weathering of silicate rocks as a function of elevation in the southern swiss Alps. *Geochimica Et Cosmochimica Acta*, 56, 3209–3216.
- Dupre, B., Dessert, C., Oliva, P., Godderis, Y., Viers, J., Francolis, L., Millot, R., & Gillardet, J. (2003). Rivers, chemical weathering and Earth's climate. *Comptes Rendus Geosciences*, 335, 1141–1160.
- Dypvik, H., & Harris, N. B. (2001). Geochemical facies analysis of fine grained siliciclastics using Th/U, Zr/Rb and (Zr + Rb)/Sr ratios. *Chemical Geology*, 181(1–4), 131–146.
- Edmond, J. M. (1992). Himalayan tectonics, weathering processes, and the strontium isotope record in marine limestones. *Science*, 258, 1594–1597.
- Fedo, C. M., Nesbitt, H. W., & Young, G. M. (1995). Unravelling the effects of potassium metasomatism in sedimentary rocks and paleosols, with implications for palaeoweathering conditions and provenance. *Geology*, 23, 921–924.
- Feng, R., & Kerrich, R. (1990). Geochemistry of the fine grained clastic sediments in the Archean Abitibi greenstone belt, Canada: Implications for provenance and tectonic setting. *Geochimica Et Cosmochimica Acta*, 54, 1061–1108.
- Floyd, P. A., Winchester, J. A., & Park, R. G. (1989). Geochemistry and tectonic setting of Lewisian clastic meta-sediments from the Early Proterozoic Loch Maree Group of Gairloch, N. W. Scotland. *Precambrian Research*, 45(1–3), 203–214.

- Galy, A., & France-Lanord, C. (2001). Higher erosion rates in the Himalaya: Geochemical constraints on riverine fluxes. *Geology*, 29, 23–26.
- Garzanti, E., Andò, S., France-Lanord, C., Censi, P., Vignola, P., Galy, V., & Lupker, M. (2011). Mineralogical and chemical variability of fluvial sediments 2. Suspended-load silt (Ganga–Brahmaputra, Bangladesh). *Earth and Planetary Science Letters*, 302, 107–120. <https://doi.org/10.1016/j.epsl.2010.11.043>.
- Garzanti, E., Andò, S., France-Lanord, C., Vezzoli, G., Censi, P., Galy, V., & Najman, Y. (2010). Mineralogical and chemical variability of fluvial sediments 1. Bedload sand (Ganga–Brahmaputra, Bangladesh). *Earth and Planetary Science Letters*, 299, 368–381. <https://doi.org/10.1016/j.epsl.2010.09.017>.
- Garzanti, E., & Resentini, A. (2016). Provenance control on chemical indices of weathering (Taiwan river sands). *Sedimentary Geology*, 336, 81–95. <https://doi.org/10.1016/j.sedgeo.2015.06.013>.
- Garzanti, E., Wang, J. G., Vezzoli, G., & Limonta, M. (2016). Tracing provenance and sediment fluxes in the Irrawaddy River basin (Myanmar). *Chemical Geology*, 440, 73–90. <https://doi.org/10.1016/j.chemgeo.2016.06.010>.
- Hayashi, K., Fujisawa, H., Holland, H. D., & Ohmoto, H. (1997). Geochemistry of 1.9 Ga sedimentary rocks from north eastern Labrador, Canada. *Geochimica Et Cosmochimica Acta*, 61, 4115–4137. [https://doi.org/10.1016/S0016-7037\(97\)00214-7](https://doi.org/10.1016/S0016-7037(97)00214-7).
- Heier, K. S., & Billings, G. K. (1970). Rubidium. In K. H. Wedepohl (Ed.), *Handbook of geochemistry*. New York: Springer.
- Herron, M. M. (1988). Geochemical classification of terrigenous sands and shales from core or log data. *Journal of Sedimentary Petrology*, 58, 820–829.
- Holail, H. M., & Moghazi, A. K. M. (1998). Provenance, tectonic setting and geochemistry of greywackes and siltstones of the Late Precambrian Hammamat Group, Egypt. *Sedimentary Geology*, 116, 227–250.
- Hossain, H. M. Z. (2019). Major, trace, and REE geochemistry of the Meghna River sediments, Bangladesh: Constraints on weathering and provenance. *Geological Journal*. <https://doi.org/10.1002/gj.3595>.
- Hossain, H. M. Z., Hossain, Q. H., Kamei, A., & Araoka, D. (2018). Compositional variations, chemical weathering and provenance of sands from the Cox's Bazar and Kuakata beach areas, Bangladesh. *Arabian Journal of Geosciences*, 11(23), 1–17. <https://doi.org/10.1007/s12517-018-4111-4>.
- Hossain, H. M. Z., Kawahata, H., Roser, B. P., Sampei, Y., Manaka, T., & Otani, S. (2017). Geochemical characteristics of modern river sediments in Myanmar and Thailand: Implications for provenance and weathering. *Chemie Der Erde*, 77, 443–458. <https://doi.org/10.1016/j.chemer.2017.07.005>.
- Kanhaiya, S., Singh, B. P., & Singh, S. (2018a). Mineralogical and Geochemical behaviour of sediments solely derived from Bundelkhand granitic complex, Central India: Implications to provenance and source rock weathering. *Geochemistry International*, 56(12), 1245–1262.
- Kanhaiya, S., Singh, B. P., Singh, S., Mitta, P., & Srivastava, V. K. (2018b). Morphometric analysis, bed-load sediments, and weathering intensity in the Khurar River Basin, Central India. *Geological Journal*. <https://doi.org/10.1002/gj.3194>.
- Khanna, P. P., Saini, N. K., Mukherjee, P. K., & Purohit, K. K. (2009). An appraisal of ICP-MS technique for determination of REEs: Long term QC assessment of Silicate rock analysis. *Himalayan Geology*, 30(1), 95–99.
- Krishnaswami, S., & Singh, S. K. (2005). Chemical weathering in the river basins of the Himalaya, India. *Current Science*, 89(5), 841–849.
- Lupker, M., France-Lanord, C., Galy, V., Lavé, J., Gaillardet, J., Gajurel, A. P., & Sinha, R. (2012). Predominant floodplain over mountain weathering of Himalayan sediments (Ganga basin). *Geochimica Et Cosmochimica Acta*, 84, 410–432. <https://doi.org/10.1016/j.gca.2012.02.001>.
- Maynard, J. B., Valloni, R., Yu, H. S. (1982) Composition of modern deep-sea sands from arc-related basins. In: Leggett JK (eds) Trench forearc geology: sedimentation and tectonics on modern and ancient active plate margins. Geological Society of London Special Publication, vol 10, pp 551–561.
- McLennan, S. M. (1989). Rare earth elements in sedimentary rocks: Influence of provenance and sedimentary processes. *Reviews in Mineralogy*, 21, 169–200.
- McLennan, S. M., Hemming, S., McDaniel, D. K., Hanson, G. N. (1993). Geochemical Approaches to Sedimentation, Provenance and Tectonics. In: Johnsson MJ, Basu A (Eds) Processes Controlling the Composition of Clastic Sediments: Geological Society of America, Special Papers, vol 285, pp 21–40.
- McLennan, S. M., Nance, W. B., & Taylor, S. R. (1980). Rare earth element–thorium correlation in sedimentary rocks and the composition of the continental crust. *Geochimica Et Cosmochimica Acta*, 44, 1833–1839.
- Mondal, M. E. A., Wani, H., & Mondal, B. (2012). Geochemical signature of provenance, tectonics and chemical weathering in the Quaternary flood plain sediments of the Hindon River, Gangetic Plain, India. *Tectonophysics*, 566–567, 87–94.
- Nesbitt, H. W., & Young, G. M. (1982). Early Proterozoic climate and plate motion inferred from major element chemistry of lutites. *Nature*, 299, 715–717.
- Nesbitt, H. W., & Young, G. M. (1984). Prediction of some weathering trends of plutonic and volcanic rocks based on thermodynamic and kinetic considerations. *Geochimica Et Cosmochimica Acta*, 48, 1523–1534.
- Nesbitt, H. W., & Young, G. M. (1989). Formation and diagenesis of weathering profiles. *Journal of Geology*, 97, 129–147.
- Nesbitt, H. W., & Young, G. M. (1996). Petrogenesis of sediments in the absence of chemical weathering: Effects of abrasion and sorting on bulk composition and mineralogy. *Sedimentology*, 43, 341–358.
- Pettijohn, F. J., Potter, P. E., & Siever, R. (1972). *Sand and sandstone* (p. 618). Berlin: Springer.
- Potter, P. E. (1978). Petrology and chemistry of modern big river sands. *Journal of Geology*, 86(4), 423–449.
- Purohit, K. K., Saini, N. K., & Khanna, P. P. (2010). Geochemical dispersion pattern of heavy metal abundances in the intermontane Pinjaur Dun, Sub-Himalaya. *Himalayan Geology*, 31(1), 29–34.
- Ramos-Vázquez, M., Armstrong-Altrin, J. S., Rosales-Hoz, L., Machain-Castillo, M. L., & Carranza-Edwards, A. (2017). Geochemistry of deep sea sediments in two cores retrieved at the mouth of the Coatzacoalcos river delta, Western Gulf of Mexico, Mexico. *Arabian Journal of Geosciences*, 10(6), 1–19. <https://doi.org/10.1007/s12517-017-2934-z>.
- Resmi, M. R., & Achyuthan, H. (2018). Lower Palar River sediments, Southern Peninsular, India: Geochemistry, source-area weathering, provenance and tectonic setting. *Journal of Geological Society of India*, 92, 83–91.
- Rollinson, H. R. (1993). *Using geochemical data: Evaluation, presentation, interpretation*. Harlow: Longman.
- Roser, B. P., Cooper, R. A., Nathan, S., & Tulloch, A. J. (1996). Reconnaissance sandstone geochemistry, provenance and tectonic setting of the lower Palaeozoic terrains of the West Coast and Nelson, New Zealand. *New Zealand Journal Geology Geophysics*, 39, 1–16. <https://doi.org/10.1080/00288306.1996.9514690>.
- Roser, B. P., & Korsch, R. J. (1986). Determination of tectonic setting of sandstone-mudstone suites using SiO<sub>2</sub> content and K<sub>2</sub>O/Na<sub>2</sub>O ratio. *Journal of Geology*, 94, 635–650. <https://doi.org/10.1086/629071>.

- Roser, B. P., & Korsch, R. J. (1988). Provenance signatures of sandstone–mudstone suites determined using discriminant function analysis of major-element data. *Chemical Geology*, *67*, 119–139. [https://doi.org/10.1016/0009-2541\(88\)90010-1](https://doi.org/10.1016/0009-2541(88)90010-1).
- Rudnick, R.L., & Gao, S. (2014). Composition of the continental crust. In R. L. Rudnick (Ed.), *Treatise on geochemistry* (eds. H. D. Holland and K. K. Turekian) (2nd ed., Vol. 4) (pp. 1 – 51. In: The crust). Oxford: Elsevier - Pergamon.
- Saini, N. K., Mukherjee, P. K., Rathi, M. S., & Khanna, P. P. (2000). Evaluation of energy dispersive X-ray fluorescence spectrometry in the analysis of silicate rocks using pressed powder pellets. *X-Ray Spectroscopy*, *29*, 166–172.
- Sensarma, S., Rajamani, V., & Tripathi, J. K. (2008). Petrography and geochemical characteristics of the sediments of the small river Hemavati, South India: Implications for provenance and weathering processes. *Sedimentary Geology*, *205*, 111–125.
- Sharma, A., Sensarma, S., Kumar, K., Khanna, P. P., & Saini, N. K. (2013). Mineralogy and geochemistry of the Mahi River sediments in tectonically active western India: Implications for Deccan large igneous province source, weathering and mobility of elements in a semi-arid climate. *Geochimica Et Cosmochimica Acta*, *104*, 63–83.
- Shapiro, L., Brannock, W. W. (1962). Rapid analysis of silicate, carbonate and phosphate rocks. U. S. Geological Survey Bulletin vol 48, pp. 49–55.
- Shaw, D. M. (1968). A review of K-Rb fractionation trends by covariance analysis. *Geochimica Et Cosmochimica Acta*, *32*(6), 573–601.
- Singh, B. P. (2000). Sediment dispersal pattern in the Murree Group of the Jammu area, NW Himalaya, India. *Himalayan Geology*, *21*, 189–200.
- Singh, B. P. (2013). Evolution of the Palaeogene succession of the western Himalayan foreland basin. *Geoscience Frontiers*, *4*, 199–212.
- Singh, B. P., Fotedar, B. K., & Rao, A. S. (1990). Petrography and geochemistry of the sandstones of Murree Group around Laren, Udhampur, Jammu Himalaya. *Geological Society of India*, *36*, 502–511.
- Singh, B. P., & Lee, Y., II. (2007). Atmospheric CO<sub>2</sub> and climate during Late Eocene on the Indian subcontinent. *Current Science*, *92*, 518–523.
- Singh, B. P., Pawar, J. S., & Karlupia, S. K. (2004). Dense mineral data from the north western Himalayan foreland sedimentary rocks and recent river sediments: Evaluation of the hinterland. *Journal of Asian Earth Sciences*, *23*, 25–35.
- Singh, P. (2009). Major, trace and REE geochemistry of the Ganga River sediments: Influence of provenance and sedimentary processes. *Chemical Geology*, *266*(3), 242–255.
- Singh, P. (2010). Geochemistry and provenance of stream sediments of the Ganga River and its major tributaries in the Himalayan region, India. *Chemical Geology*, *269*, 220–236.
- Singh, P., & Rajamani, V. (2001a). Geochemistry of the Kaveri flood-plain sediments, Southern India. *Journal of Sedimentary Research*, *71*(1), 50–60.
- Singh, P., & Rajamani, V. (2001b). REE geochemistry of recent clastic sediments from the Kaveri floodplains, southern India: Implication to source area weathering and sedimentary processes. *Geochimica Et Cosmochimica Acta*, *65*, 3093–3108.
- Singh, R. (2007). Geology of Kishtwar Region, Jammu & Kashmir Himalaya, India with special emphasis on the Salkhalas, Central Crystallines; Their relationship and implication on Main Central Thrust. *Journal of Geological Society of India*, *69*, 699–709.
- Sinha, S., Islam, R., Ghosh, S. K., Kumar, R., & Sangode, S. J. (2007). Geochemistry of Neogene Siwalik mudstone along Punjab re-entrant, India: Implication for source-area weathering, provenance and tectonic setting. *Current Science*, *92*(8), 1103–1113.
- Stork, A. L., Smith, D. K., & Gill, J. B. (1987). Evaluation of geochemical reference standards by X-ray fluorescence analysis. *Geo-standards Newsletter*, *11*, 107–113.
- Strahler, A. N. (1969). *Physical geography* (3rd ed.). New York: Wiley.
- Sun, Q., Wang, S., Zhou, J., Chen, Z., Shen, J., Xie, X., Wu, F., & Chen, P. (2010). Sediment geochemistry of Lake Daihai, north-central China: Implications for catchment weathering and climate change during the Holocene. *Journal of Paleolimnology*, *43*, 75–87.
- Suttner, L. J., & Dutta, P. K. (1986). Alluvial sandstone composition and palaeoclimate; I, Framework mineralogy. *Journal of Sedimentary Research*, *56*(3), 329–345.
- Taylor, S. R., & McLennan, S. M. (1985). *The continental crust: Its composition and evolution*. Oxford: Blackwell.
- Thakur, V. C., Rawat, B. S., & Islam, R. (1990). Zanskar crystalline—Some observations on its lithostratigraphy, deformation, metamorphism and regional framework. *Himalayan Geology*, *1*, 11–25.
- Tripathi, J. K., & Rajamani, V. (2003). Geochemistry of Delhi quartzites: Implications for the provenance and source area weathering. *Journal of Geological Society of India*, *62*, 215–226.
- Tripathy, G. R., Singh, S. K., & Ramaswamy, V. (2014). Major and trace element geochemistry of Bay of Bengal sediments: Implications to provenances and their controlling factors. *Paleogeography, Paleoclimatology, Paleoecology*, *397*, 20–30.
- Verma, M., Singh, B. P., Srivastava, A., & Mishra, M. (2012). Chemical behavior of suspended sediments in a small river draining out of the Himalayan Orogenic Belt, Northern India. *Himalayan Geology*, *33*(1), 1–14.
- Verma, S. P., & Armstrong-Altrin, J. S. (2013). New multi-dimensional diagrams for tectonic discrimination of siliciclastic sediments and their application to Precambrian basins. *Chemical Geology*, *355*(5), 117–133. <https://doi.org/10.1016/j.chemgeo.2013.07.014>.
- Wronkiewicz, D. J., & Condie, K. C. (1989). Geochemistry and provenance of sediments from the Pongola Supergroup, South Africa: Evidence for a 3.0 Ga. Old continental craton. *Geochimica Et Cosmochimica Acta*, *53*, 1537–1549.

**Publisher's note** Springer Nature remains neutral with regard to jurisdictional claims in published maps and institutional affiliations.